

VALIDATION OF TWO TURBULENT FLAME SPEED CLOSURE MODELS FOR SLOW AND FAST HYDROGEN DEFLAGRATION

T. Holler¹, V. Jain², and E.M.J. Komen²

¹ Reactor Engineering Division, Jožef Stefan Institute (JSI),
Jamova cesta 39, SI-1000, Ljubljana, Slovenia

² Nuclear Research and Consultancy Group (NRG),
Westerduinweg 3, 1755 ZG, Petten, the Netherlands
tadej.holler@ijs.si; v.jain@nrg.eu; komen@nrg.eu

ABSTRACT

Hydrogen is a flammable gas that can be generated during a severe accident in a Light Water Reactor. Hydrogen combustion in the containment may damage relevant safety systems and the containment wall. The potential risk of hydrogen can be assessed using Computational Fluid Dynamics (CFD) modeling. This paper presents CFD modeling validation against fast deflagration experiments performed in the ENACEFF facility and slow deflagration experiments conducted in the THAI facility. Validation was performed for two flame speed closure combustion models. One based on the works of Zimont, i.e. the Turbulent Flame Closure (TFC) model, and one based on the works of Lipatnikov, i.e. the Flame Speed Closure (FSC) model. The presented validation results show good performance of the implemented combustion models both qualitatively and quantitatively. Moreover, the Zimont combustion model showed superior accuracy in the ENACCEF tests, where fast deflagration occurs, whereas the Lipatnikov combustion model indicated improvement in the initial stages of slow deflagration regime in the THAI experiments.

KEYWORDS

Hydrogen, Premixed turbulent combustion, Turbulent flame closure model, Flame speed closure model

1. INTRODUCTION

The production and release of hydrogen into the containment during a severe accident is an important safety issue for Light Water Reactors (LWRs) [1]. Combustion of hydrogen may cause structural damage to the containment and may compromise its function as final barrier for release of radioactive fission products to the environment. To reduce the hydrogen risk as far as possible, hydrogen mitigation systems such as Passive Auto-catalytic Recombiners (PARs) and igniters can be installed. Computer modeling is required to demonstrate the adequacy of the Nuclear Power Plant's (NPP's) hydrogen risk management system. The topic received increased attention following the Three Mile Island accident in the USA back in 1979 [2] and the accident in the Japanese Fukushima Daiichi NPP in March of 2011 [3]. Computer modeling is required for the optimal design of hydrogen mitigations systems and the assessment of the accompanied residual risks of the presence of hydrogen. Complementary to the use of so-called lumped parameter codes, Computational Fluid Dynamics (CFD) modeling can be used for more detailed assessment of the hydrogen risks. For that purpose, extensive validation of CFD is a prerequisite.

A series of papers on the topic of combustion modeling in hydrogen safety management based on NRG's CFD-based modeling has been presented. In the first paper of Sathiah et al. [4], the combustion model based on the work of Zimont [5] was introduced, which is implemented using User Defined Functions

(UDF) in the ANSYS Fluent code [6]. The applied modeling approach incorporates the application of Adaptive Mesh Refinement (AMR), in order to accurately and efficiently track the turbulent flame propagation. In the first work, the model was validated against small scale experiments with methane-air mixtures. In the subsequent two papers, the modeling approach has been validated against fast deflagration experiments in uniform hydrogen-air [7] and in uniform hydrogen-air-CO₂-He mixtures [8], respectively, as performed in the ENACCEF facility [9, 14]. The validations of that model were further extended in the fourth paper [10], for non-uniform hydrogen-air mixture experiments in the ENACCEF facility. The general conclusion from all those validations was that the model predicts the intermediate peak pressure, the maximum pressure, the pressure increase rate, and the eigen frequencies with their amplitudes of the residual pressure wave phenomena from the ENACCEF experiments quite well. However, some overpredictions of the flame propagation velocity during the initial quasi-laminar flame propagation regime were observed. The model was further extended with an additional laminar source term in the combustion model based on the work of Lipatnikov and Chomiak [11]. This extended combustion model was validated against experiments performed in the large scale THAI experimental facility [12] in the latest paper of the series [13]. The results showed clear advantage of the Lipatnikov model in the initial quasi-laminar regime.

Therefore, the objective of this paper is to compare the performance of the Zimont combustion model and the Lipatnikov combustion model against both the fast deflagration experimental results obtained from ENACCEF facility and the slow deflagration experimental results from the THAI facility.

This paper is structured as follows: the considered experimental results and the corresponding experimental facilities are presented in the Section 2, followed by the introduction of the applied CFD combustion models of Zimont and Lipatnikov in Section 3. The results are presented and discussed in Section 4 and finally summarized and concluded in Section 5.

2. EXPERIMENTS

Experimental results selected for our validation came from two experimental facilities (Figure 1) presented in this section, with the initial hydrogen concentrations, temperature, pressures and blockage ratios of these experiments shown in Table I. The blockage ratio, BR , is defined as $BR = 1 - (d/D)^2$, where d and D are baffle and pipe diameters, respectively. All considered experiments were conducted using uniform mixtures of hydrogen and air. Only the essential details of the considered experiments, necessary for the understanding of the presented simulations, are provided in this paper.

2.1. ENACCEF Experimental Vessel

The ENACCEF facility, which is shown in Figure 1 (left), is located in Orleans, France, and is operated by the French National Centre for Scientific Research (Centre national de la recherche scientifique – CNRS). It is a vertical facility consisting of two parts. The first part is a 3.2 m long acceleration tube with diameter of 0.154 m in which various obstacles can be inserted to induce turbulence. The second part is a dome with height of 1.7 m and diameter of 0.738 m and a total volume of 0.658 m³. The ENACCEF facility is capable of producing very fast deflagrations thanks to inserted baffles in the acceleration tube. It is equipped with detectors to measure flame propagation velocity and pressure build-up inside the vessel during combustion, as well as with gas mixture sampling probes at various locations along the vessel.

In a benchmark exercise within the Severe Accident Research Network of Excellence (SARNET, 7th Framework Programme of the European Commission, 2009-2013) [14], three experiments with different blockage ratios were used. Results of two of those experiments are used in the scope of this paper, with initial conditions provided in Table I.

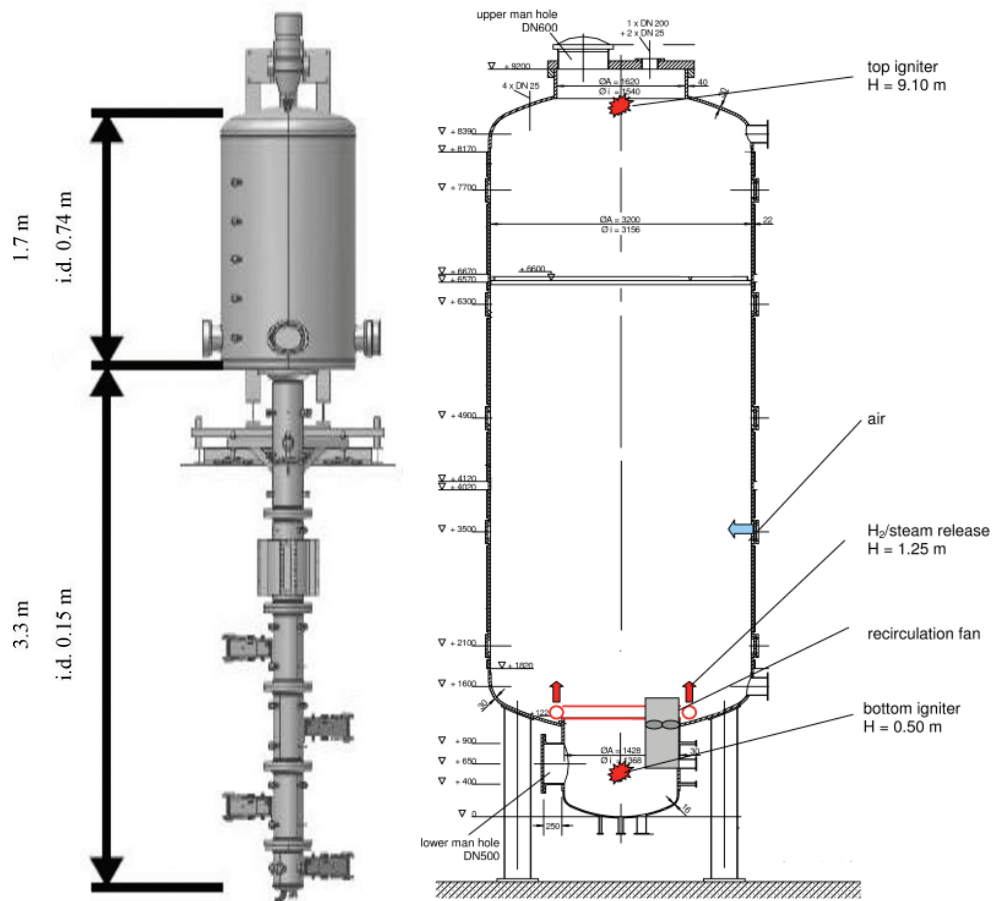


Figure 1. Schematics of the ENACCEF experimental vessel (left) and the THAI experimental vessel (right).

Table I. Initial conditions of considered experiments.

	Hydrogen concentration [vol. %]	Temperature [K]	Pressure [kPa]	Blockage ratio []	Mixture
ENACCEF RUN 153	13.0	296.0	100.0	0.63	Uniform
ENACCEF RUN 158	13.0	296.0	100.0	0.33	Uniform
THAI HD-12	8.0	291.0	148.5	0.00	Uniform
THAI HD-3	9.0	295.5	148.5	0.00	Uniform

2.2. THAI Experimental Vessel

The THAI containment test facility, shown in Figure 1 (right), is operated by Becker Technologies GmbH in Eschborn, Germany. It is a vertical cylindrical stainless steel vessel designed to withstand pressures of 20 bar at wall temperature 20 °C. The facility is measuring 9.2 m in height and 3.2 m in diameter, bringing the total volume to 60 m³. Within the framework of the hydrogen deflagration (HD) part of the OECD-NEA THAI project [12], 29 different experiments were performed, aiming to provide a deeper

insight into the phenomenology of hydrogen deflagrations. In these experiments, varying initial conditions were used, by changing the initial hydrogen and steam concentrations, temperature, pressure, ignition location, and atmosphere stratification. During these experiments, all inner structures that could possibly induce turbulence were removed, except for the experimental instrumentation, which consisted of 43 thermocouples and 4 pressure transducers distributed throughout the vessel.

For the purpose of this paper, two experiments with bottom ignition and different hydrogen concentrations were selected. The initial conditions of these experiments are presented in Table I.

3. NUMERICAL APPROACH

The ANSYS Fluent CFD code was used as a platform to implement our hydrogen combustion model. On top of the equations for conservation of mass, momentum and energy, the additional transport equation for the Favre-averaged progress variable, \tilde{c} , is resolved. This progress variable is defined as:

$$\tilde{c} = \frac{\tilde{Y}_f - Y_{f,u}}{Y_{f,b} - Y_{f,u}} \quad (1)$$

Here Y_f is the mass fraction of fuel, with indexes u and b representing the unburned and burned state, respectively. For solving these equations, the density-based coupled solver was used in ANSYS Fluent, together with an explicit time stepping method. The turbulence model used in computations is the standard $k - \varepsilon$ model.

In order to obtain accurate results, while maintaining computational times at reasonable levels, an adaptive mesh refinement (AMR) technique was used. For the presented simulation results two levels of AMR were used on top of a base grid, which was shown to be sufficient to yield grid independent results in our previous work [7, 13]. Each level of refinement means halving the size of a computational cell in every direction of the axisymmetric 2D model used in our calculations. For the ENACCEF tests, the base grid used was around 1 cm by 1 cm, whereas the base grid was slightly larger for the THAI tests, measuring roughly 4 cm by 4 cm.

While adiabatic walls were prescribed as thermal boundary conditions for tests in the ENACCEF facility, tests in the THAI experimental facility were computed using prescribed constant wall temperature and the Discrete Ordinates (DO) thermal radiation model. For slow deflagration in the THAI vessel, it was shown in our previous work [13] that convection and radiation have a significant impact on total energy levels and consequently on the pressure build-up. Since the total combustion time in the ENACCEF experiments is significantly shorter than in the THAI experiments, heat transfer between walls and the gaseous mixture in the ENACCEF vessel was not accounted for in simulations. Thermal radiation was neglected as well in the computations of the ENACCEF experiments.

The following subsection presents the two applied combustion models and the corresponding progress variable transport equations which have been implemented in the ANSYS Fluent via user defined functions (UDF) for the considered simulations.

3.1. Zimont Combustion Model

Zimont [5] used the following progress variable transport equation:

$$\frac{\partial \bar{\rho} \tilde{c}}{\partial t} + \frac{\partial \bar{\rho} \tilde{c} \tilde{u}_j}{\partial x_j} = \frac{\partial}{\partial x_j} \left[\bar{\rho} (\kappa + D_t) \frac{\partial \tilde{c}}{\partial x_j} \right] + \rho_u U_t |\nabla \tilde{c}| \quad (2)$$

In equation (2), κ and D_t are molecular and turbulent diffusivities, respectively, ρ_u is the unburned gas density. The turbulent burning velocity U_t is modeled by Zimont [5] as follows:

$$U_t = Au'Da^{1/4}F(Le) \quad (3)$$

Here A is a model constant, u' is the turbulent intensity and Da is the Damkohler number. Preferential diffusion thermal (PDT) instabilities were accounted for using the $F(Le)$ term [7]. This combustion model is also called the Turbulent Flame Closure (TFC) model. In this paper it will be referred to as the Zimont combustion model, which was developed for fully turbulent premixed flames.

3.2. Lipatnikov Combustion Model

To improve the model and make it valid also in weakly turbulent premixed flames, e.g. initial stages of slow deflagrations, Lipatnikov and Chomiak [11] proposed the following progress variable transport equation:

$$\frac{\partial \bar{\rho} \tilde{c}}{\partial t} + \frac{\partial \bar{\rho} \tilde{c} \tilde{u}_j}{\partial x_j} = \frac{\partial}{\partial x_j} \left[\bar{\rho} (\kappa + D_t) \frac{\partial \tilde{c}}{\partial x_j} \right] + \frac{(S_l)^2}{4(\kappa + D_t)} \rho_u \tilde{c} (1 - \tilde{c}) + \rho_u U_t |\nabla \tilde{c}| \quad (4)$$

Here S_l represents the laminar flame speed. The third term on the right hand side of equation (4) is an additional quasi-laminar term added to the progress variable transport equation (2). The turbulent burning velocity U_t is modelled using equation (3), as in the TFC combustion model. In the planar, fully developed case, the added source term results in the simple expression for the flame speed, $S_t = S_l + U_t$. The combustion model using this progress variable transport equation is also called Flame Speed Closure (FSC) model. Here it will be referred to as the Lipatnikov combustion model.

4. RESULTS AND DISCUSSION

This section presents results obtained using the Zimont and Lipatnikov combustion models based on and compared to the experiments conducted in the ENACCEF and THAI experimental facilities. The initial conditions of the selected experiments are provided in Table I. Grid independence analyses for computations in the ENACCEF and THAI facilities were performed in our previous work [7, 13], where it was shown that two levels of AMR are sufficient to give practically grid independent results for both given base grids.

The parameters of primary interest for subsequent containment integrity analysis are the maximum pressure, rate of pressure increase, and turbulent flame propagation. In the ENACCEF tests, also the eigen frequencies and amplitudes of the residual pressure waves following complete burning are of interest.

4.1. Results Based on ENACCEF Experiments

Simulations based on two different ENACCEF experiments, i.e. RUN 153 and RUN 158, were performed using the Zimont and Lipatnikov combustion models.

Results for flame position and corresponding flame propagation velocity for the ENACCEF RUN 153 are shown in Figure 2. Here it can be observed that, using the Zimont combustion model, the flame starts to propagate sooner than when the Lipatnikov model was used. Moreover, the flame propagation velocities are overpredicted by the Zimont model by more than 20 % and underpredicted by the Lipatnikov model by around 10 %. Similar observations can be made for the first pressure peak, the first rate of pressure increase, and also the maximum pressure, as shown in Figure 3 (left) and Table II. However, both combustion models are overpredicting the second rate of pressure increase quite significantly for

RUN 153, as can be seen in Table II. From Figure 3 (right), it can also be observed, that the eigen frequencies of the pressure oscillations are reproduced quite well by both combustion models. The amplitudes of these oscillations are slightly underpredicted by the Zimont model and substantially underpredicted by the Lipatnikov model.

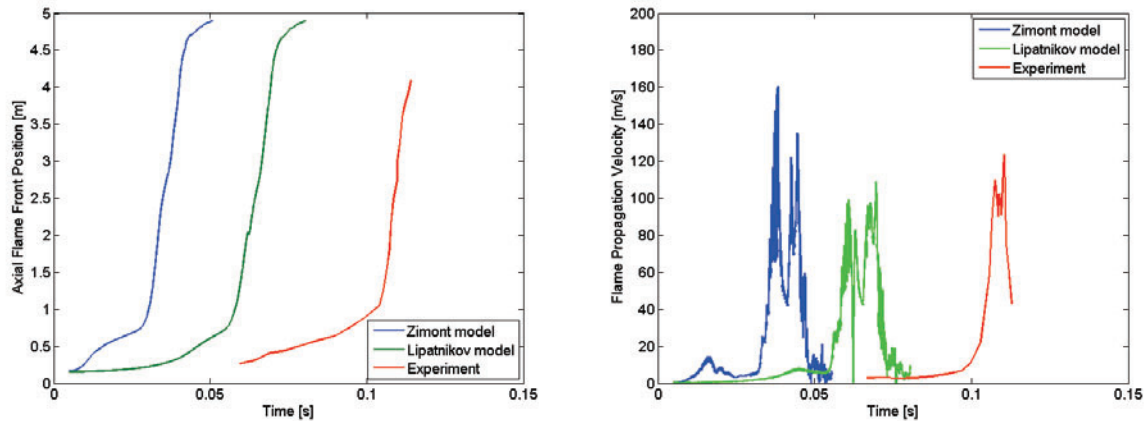


Figure 2. Flame front position (left) and flame propagation velocity results (right) for ENACCEF RUN 153. Results are shown for the Zimont and Lipatnikov combustion model, compared to experimental results.

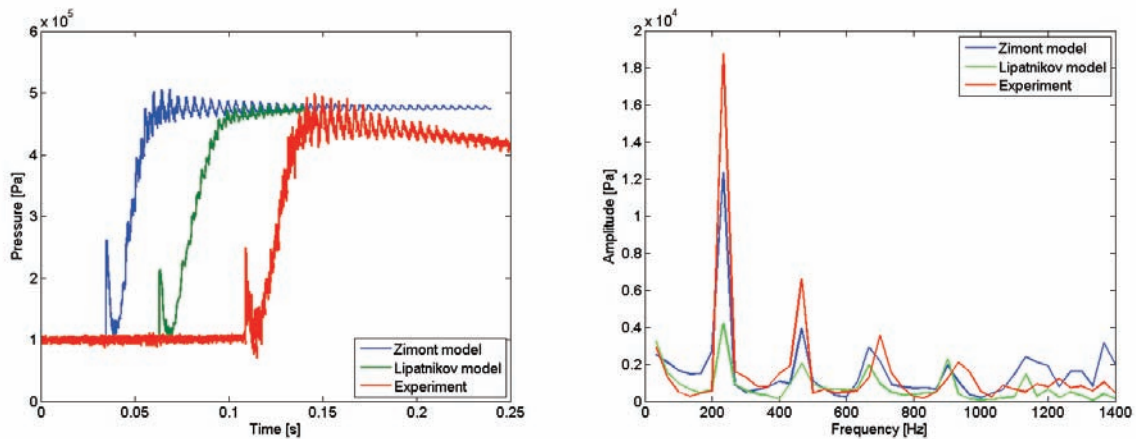


Figure 3. Pressure history (left) and eigen frequency analysis (right) results for ENACCEF RUN 153. Results are shown for the Zimont and Lipatnikov combustion model, compared to experimental results.

Table II. Results for ENACCEF RUN 153.

	Experiment	Zimont model	Difference	Lipatnikov model	Difference
Maximum pressure	$4.99 \cdot 10^5$ Pa	$5.10 \cdot 10^5$ Pa	+2.4%	$4.81 \cdot 10^5$ Pa	-3.5%
First pressure peak	$2.49 \cdot 10^5$ Pa	$2.67 \cdot 10^5$ Pa	+7.2%	$2.14 \cdot 10^5$ Pa	-14.0%
First rate of pressure increase	$1.30 \cdot 10^9$ Pa/s	$1.36 \cdot 10^9$ Pa/s	+5%	$0.81 \cdot 10^9$ Pa/s	-38%
Second rate of pressure increase	$1.18 \cdot 10^8$ Pa/s	$1.67 \cdot 10^8$ Pa/s	+42%	$1.47 \cdot 10^8$ Pa/s	+25%

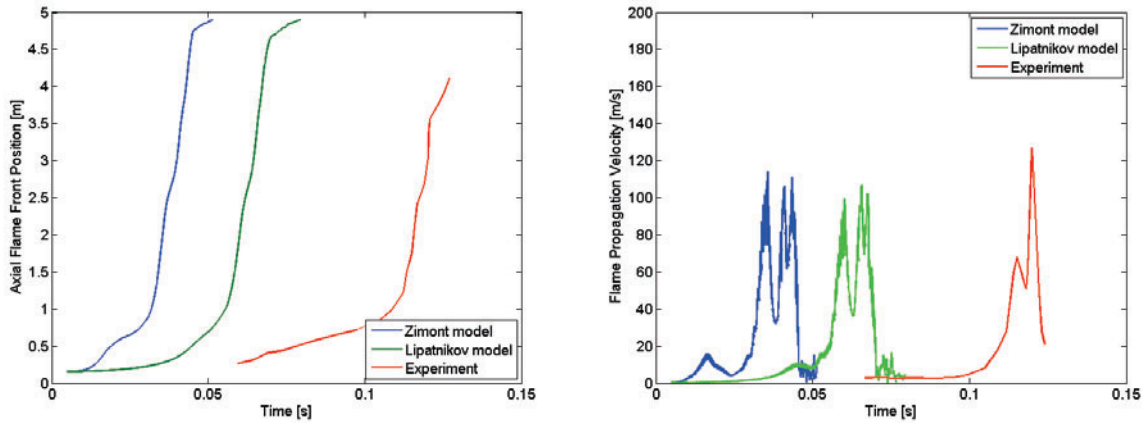


Figure 4. Flame front position (left) and flame propagation velocity results (right) for ENACCEF RUN 158. Results are shown for the Zimont and Lipatnikov combustion model, compared to experimental results.

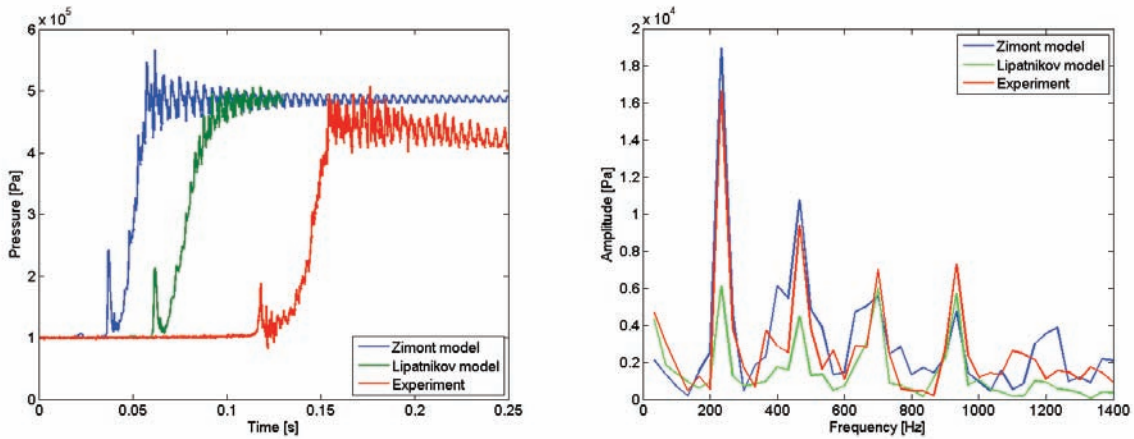


Figure 5. Pressure history (left) and eigen frequency analysis (right) results for ENACCEF RUN 158. Results are shown for the Zimont and Lipatnikov combustion model, compared to experimental results.

Similarly as for RUN 153, the flame also starts propagating sooner using the Zimont model than using the Lipatnikov model in RUN 158, as can be seen in Figure 4. However, both combustion models are underpredicting the flame propagation velocity slightly in RUN 158, as shown on the right side of Figure 4.

The maximum pressure is predicted very accurately for RUN 158 by the Lipatnikov model and is somewhat overpredicted by the Zimont model, which can be seen from Figure 5 (left) and Table III. The first pressure peaks are overpredicted by both models, while both rates of pressure increase are substantially underpredicted. The eigen frequencies of the pressure oscillations are captured very well by both models, as seen in Figure 5 (right). The amplitudes of the oscillations are again substantially underpredicted by the Lipatnikov model, while the Zimont model gives slightly overpredicted results.

Table III. Results for ENACCEF RUN 158.

	Experiment	Zimont model	Difference	Lipatnikov model	Difference
Maximum pressure	$5.07 \cdot 10^5$ Pa	$5.66 \cdot 10^5$ Pa	+11.6%	$5.06 \cdot 10^5$ Pa	-0.2%
First pressure peak	$1.88 \cdot 10^5$ Pa	$2.42 \cdot 10^5$ Pa	+28.8%	$2.13 \cdot 10^5$ Pa	+13.3%
First rate of pressure increase	$1.25 \cdot 10^9$ Pa/s	$0.80 \cdot 10^9$ Pa/s	-36.2%	$0.45 \cdot 10^9$ Pa/s	-63.9%
Second rate of pressure increase	$9.17 \cdot 10^7$ Pa/s	$4.36 \cdot 10^7$ Pa/s	-52.4%	$7.83 \cdot 10^7$ Pa/s	-14.7%

For the considered simulations based on the ENACCEF experiments, both models are predicting the considered experiments quite well. However, the Zimont combustion model can be considered superior to the Lipatnikov model regarding the prediction of the amplitudes of the pressure oscillations.

4.2. Results Based on THAI Experiments

The performance of the Zimont and Lipatnikov combustion models was also tested against the THAI HD-12 and HD-3 experiments. All computational results were obtained using constant wall temperatures, which were set equal to the initial gas temperature. Thermal radiation was modeled using the DO thermal radiation model.

The flame propagation results were deduced from the times of flame arrival to each thermocouple. There were 13 thermocouples located at different heights in the central axis of the vessel. These 13 locations represent a relatively scarce resolution for the results of the axial flame front position, and consequently, the axial flame propagation velocity. The remaining 30 thermocouples were placed off-center at 10 different heights and three different angles. It should be noted, however, that all of these off-centered thermocouples were located at the same radial distance from the center axis. Therefore, little information on radial flame propagation could be deduced from these experiments.

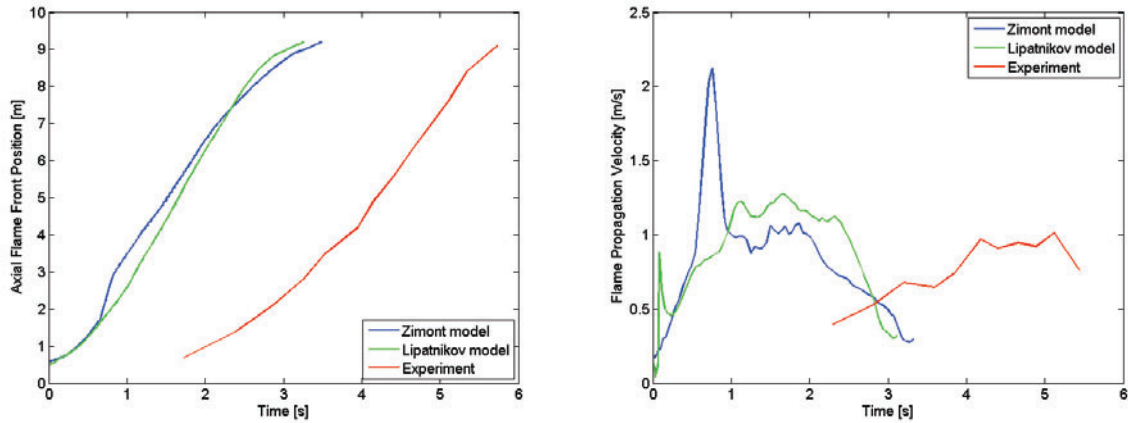


Figure 6. Flame front position (left) and flame propagation velocity results (right) for the THAI HD-12 test. Results are shown for the Zimont and Lipatnikov combustion model, compared to experimental results.

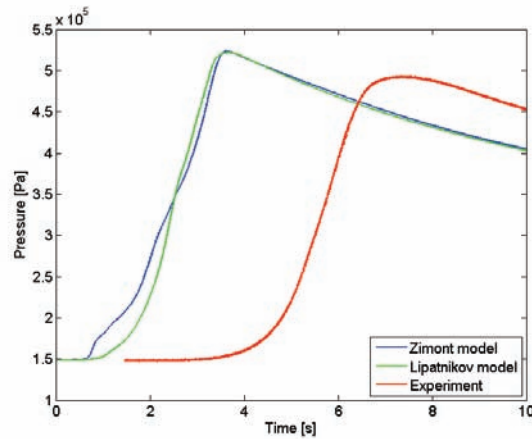


Figure 7. Pressure history results for the THAI HD-12 test. Results are shown for the Zimont and Lipatnikov combustion model, compared to experimental results.

Table IV. Results for THAI HD-12 test.

	Experiment	Zimont model	Difference	Lipatnikov model	Difference
Maximum pressure	$4.93 \cdot 10^5$ Pa	$5.23 \cdot 10^5$ Pa	+6.1%	$5.22 \cdot 10^5$ Pa	+5.8%
Rate of pressure increase	$2.09 \cdot 10^5$ Pa/s	$2.56 \cdot 10^5$ Pa/s	+22.6%	$2.35 \cdot 10^5$ Pa/s	+12.5%

Similar flame propagation was predicted for the THAI HD-12 test with the Zimont and Lipatnikov combustion models, as shown in Figure 6 (left). The Zimont model shows a slight acceleration in the initial quasi-laminar stage compared to the Lipatnikov model. This results in higher flame propagation velocity predicted by Zimont model, which can be seen in Figure 6 (right) and also in faster initial

pressure increase, shown in Figure 7. The maximum pressure is predicted quite accurately, while the rate of pressure increase is overpredicted by both models, as shown in Figure 7 and Table IV.

Figure 8 shows the predicted flame front position and velocity for the THAI HD-3 test. Again the flame propagation velocity predicted with the Zimont model is substantially higher than the one predicted with the Lipatnikov model, especially in the initial quasi-laminar stage. However, both Zimont and Lipatnikov combustion models predict the maximum flame propagation velocity in the initial stages of combustion, whereas in the experiment, the maximum was detected at the end. The pressure history shown in Figure 9 indicates that some pressure oscillations observed in experiment were not captured by the models. These oscillations result in a faster pressure increase and a higher maximum pressure than predicted by the combustion models, as shown in Table V. Similarly to the test HD-12, it can be noted in Figure 9, that while the initial pressure increase is overpredicted by both combustion models, it is substantially faster using the Zimont model.

For the simulations of the considered THAI experiments both combustion models were reasonably accurate regarding maximum pressure prediction. However, the Lipatnikov model displayed better accuracy regarding the initial quasi-laminar regime, which takes place in initial stages of slow deflagration, as was also one of the initial theoretical assumptions for developing that combustion model.

Table V. Results for THAI HD-3 test.

	Experiment	Zimont model	Difference	Lipatnikov model	Difference
Maximum pressure	$5.77 \cdot 10^5$ Pa	$5.42 \cdot 10^5$ Pa	-6.1%	$5.51 \cdot 10^5$ Pa	-4.5%
Rate of pressure increase	$7.36 \cdot 10^5$ Pa/s	$4.49 \cdot 10^5$ Pa/s	-39.0%	$3.06 \cdot 10^5$ Pa/s	-58.5%

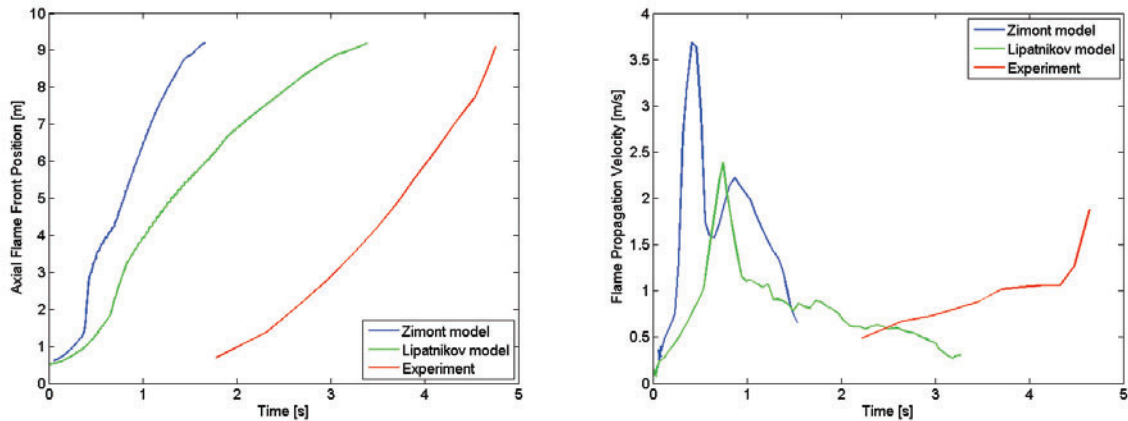


Figure 8. Flame front position (left) and flame propagation velocity results (right) results for the THAI HD-3 test. Results are shown for the Zimont and Lipatnikov combustion model, compared to experimental results.

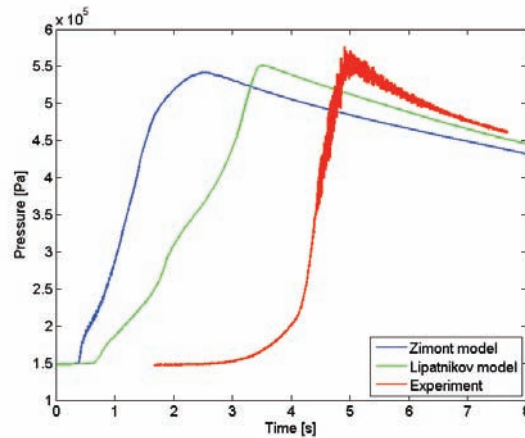


Figure 9. Pressure history results for the THAI HD-3 test. Results are shown for the Zimont and Lipatnikov combustion model, compared to experimental results.

5. SUMMARY AND CONCLUSION

The hazard of possible hydrogen release and combustion during a severe accident in LWR NPP can be investigated using CFD-based modeling. For this paper, two flame speed combustion models, developed by Zimont and Lipatnikov, were implemented in the ANSYS Fluent CFD code and were validated against fast deflagration in the ENACCEF facility and a slow deflagration in the THAI facility.

Both combustion models performed quite well for the considered experiments. However, the Zimont combustion model gave better agreement for the ENACCEF experiments, where deflagration is fast and occurs in fully turbulent premixed regimes. The main advantage of this combustion model is the accurate prediction of the eigen frequencies and amplitudes of the residual pressure waves, which occur after complete combustion. On the other hand, the Lipatnikov combustion model, with its additional source term in equation (4), performs better for the initial quasi-laminar stages of slow deflagration in the THAI experiments, which take place in low turbulence regimes. This additional term, however, seems to act as a dumping factor for the pressure oscillations in deflagrations occurring in the fully developed turbulent combustion present in the ENACCEF experimental vessel. Therefore, when choosing between the Zimont and Lipatnikov combustion models, one has to be aware of advantages and deficiencies of both models. One also has to choose accordingly to the anticipated deflagration regime in which the majority of combustion will take place.

Further validation of the considered hydrogen deflagration modeling is required, before it can be applied to the analysis of possible hydrogen deflagrations in real-scale NPP containments. For this purpose, a next step is to validate these models against experiments of hydrogen combustion conducted in even larger experimental facilities than the THAI facility. This effort is currently being undertaken and will be presented in the near future. The presented CFD modeling approach, along with the solid validation base presented so far is considered to be a promising route towards the analysis of the potential hazard of the hydrogen deflagration in the containment of an NPP during a severe accident.

ACKNOWLEDGEMENTS

The work described in this paper was funded by the Dutch Ministry of Economic Affairs and by the Slovenian Research Agency (ARRS) with research program "Reactor engineering" and research project "Experiment and simulation of hydrogen combustion in nuclear power plant containment experimental facility".

REFERENCES

1. I. Kljenak, A. Bentaib and T. Jordan, 2012. Hydrogen behavior and control in severe accidents, in: Nuclear Safety in Light Water Reactors, B. R. Sehgal ed., pp. 186-227, Elsevier, 2012.
2. “Report of the President’s Commission on The Accident at Three Mile Island”, U.S. Government Printing Office, Washington D.C., USA, 1979.
3. “Fukushima Daiichi: ANS Committee Report”, American Nuclear Society Special Committee, Illinois, USA, 2012.
4. P. Sathiah, E. Komen and D. Roekaerts, “The role of CFD combustion modeling in hydrogen safety management—Part I: Validation based on small scale experiments”, *Nuclear Engineering and Design*, vol. 248, pp. 93-107, 2012.
5. V.L. Zimont, “Theory of turbulent combustion of a homogenous fuel mixture at high Reynolds number”, *Combust. Explos. Shock Waves*, vol. 15, pp. 305–311, 1979.
6. ANSYS Fluent. ANSYS-Fluent Inc., 2008 ANSYS-Fluent Inc., 2008. Fluent 12.0. Lebanon, N.H., 2008
7. P. Sathiah, S. van Haren, E. Komen and D. Roekaerts, “The role of CFD combustion modeling in hydrogen safety management—II: Validation based on homogeneous hydrogen–air experiments”, *Nuclear Engineering and Design*, vol. 252, pp. 289-302, 2012.
8. P. Sathiah, E. Komen and D. Roekaerts, “The role of CFD combustion modeling in hydrogen safety management-III: Validation based on homogeneous hydrogen-air-diluent experiments“, *Nuclear Engineering and Design*, In press, 2014.
9. OECD/NEA report, “ISP-49 on Hydrogen Combustion”, NEA/CSNI/R(2011)9, 2012.
10. P. Sathiah, E. Komen and D. Roekaerts, “The role of CFD combustion modeling in hydrogen safety management-IV: Validation based on non-homogeneous hydrogen-air experiments“, Submitted to Nuclear Engineering and Design, 2014.
11. A.N. Lipatnikov and J. Chomiak, “Turbulent flame speed and thickness: phenomenology, evaluation, and application in multi-dimensional simulations”, *Progress in Energy and Combustion Science*, vol. 28, no. 1, pp. 1-74, 2002.
12. T. Kanzleiter and G. Langer, “Hydrogen Deflagration Tests in the THAI Test Facility”, Becker Technologies GmbH, Eschborn, Germany, Tech. Rep. 150 1326–HD-2, 2010.
13. P. Sathiah, T. Holler, I. Kljenak, and E. Komen, “The role of CFD combustion modeling in hydrogen safety management-V: Validation for slow deflagrations in homogeneous hydrogen-air experiments“, Submitted to Nuclear Engineering and Design, 2015.
14. A. Bentaib et al., “SARNET hydrogen deflagration benchmarks: Main outcomes and conclusions”, *Annals of Nuclear Energy* 74, pp. 143-152, 2014